Multi-Mode Broadband Power Transfer through a Wire Medium Slab

**Dmytro Vovchuk[1, 2], Sergei Kosulnikov[1, 3, *], Igor Nefedov[1],
Sergei Tretyakov[1], and Constantin Simovski[1, 3]**

(*Invited Paper*)

Abstract—It is known that slabs of wire media — dense arrays of thin conducting wires — can transport electromagnetic energy of evanescent plane waves over the slab thickness. This phenomenon was successfully used in superlenses and endoscopes. However, in the known configurations the effective energy transfer takes place only at the Fabry-Perot (thickness) resonances of the slab, making broadband power transfer impossible. In this paper we experimentally demonstrate that power transfer by a wire medium slab can be very broadband, whereas the Fabry-Perot resonances are damped, provided that the wires of the wire medium slab extend into the power-emitting body. As a testbed system we have used two rectangular waveguides and demonstrated that a properly designed and positioned wire medium slab transfers modes of any polarization from the input to the output waveguides. This study is relevant to emerging applications where broadband transport of reactive-field energy is required, especially in enhancing and controlling radiative heat flows in thermophotovoltaic systems.

1. INTRODUCTION

Wire metamaterials attract attention of researchers because these media can be used in many applications, covering a huge range of frequencies from microwaves to visible light [1]. Among various known topologies, the simple wire media (WM) — arrays of parallel metal wires either completely located in a dielectric matrix or partially free standing — are, probably, most popular due to their relatively simple design and easy manufacturing. Their remarkable property is strong and low-frequency spatial dispersion [2, 3] which is a prerequisite of the so-called canalization regime of wave propagation [4–7]. This regime holds in WM slabs whose wires are orthogonal to the interfaces. In the canalization regime all incident TM-polarized (transverse magnetic with respect to the wire axis) waves are converted at the illuminated side of the WM slab onto TEM (transverse electromagnetic, for perfectly conducting wires) or quasi-TEM (for wires with finite conductance) eigenmodes of the infinite WM. These eigenwaves propagate along the wires and are converted back to TM-waves at the rear side of the slab. Strong spatial dispersion inherent to WM allows all the excited eigenwaves to have the same group and phase velocity. Therefore, the field distribution carried by the incident wave package is transmitted across the slab practically without distortion. Not only propagating TM-waves impinging the WM slab convert into TEM-modes, so do evanescent TM-waves, too. Therefore, the canalization creates at the rear side of the WM slab a subwavelength image of a radiating or scattering object located at the front side [1, 4–8]. The object field distribution remains undistorted and strong in the amplitude even if the slab is as thick as several wavelengths [6–8].

Definitely, canalization of the wave package prevents its divergence and implies an efficient power transfer across the slab. However, this transfer is very narrowband with respect to the frequency, because canalization occurs only at the Fabry-Perot resonances of the wire-medium slab [1, 4–9]. Beyond these resonances, impedance mismatch results in strong reflections from the slab, and the TEM eignemodes are excited weakly and have a non-uniform spatial spectrum [5, 7]. One may think that WM allows efficient energy transfer only within narrow bands of resonance frequencies.

However, in works [10–12] it was theoretically predicted that broadband energy transfer through a WM slab is possible, if the wires extend into the volume of the radiating object. The effect is useful for so-called thermophotovoltaic systems [13–15]. Recent studies of nanowire-based systems confirmed strong enhancing of near-field thermal radiation [16, 17]. Metal nanowires filling a vacuum gap between two surfaces — a hot surface of a thermal emitter and a cold surface of a semiconductor — strongly enhance the radiative heat transfer from the emitter to the semiconductor. This effect in accordance to [10–12] theoretically results from the conversion of evanescent TM-polarized waves created by the emitter into quasi-TEM waves propagating along the nanowires. As a result, very high spatial harmonics normally concentrated at the emitter surface become propagating and carry significant additional energy. Moreover, it is believed [10–12] that the broadband power transfer through the WM slabs results only from the conversion of evanescent waves into propagating ones. However, in a semitransparent emitter there exist also propagating waves. Their power transfer through the WM slab is believed to be narrowband and linked to Fabry-Perot resonances. However, is it really so? The main question which we address in this paper reads: Can the power transfer through a WM slab be efficient and broadband, especially in the case when the incident field is a usual wave beam (i.e., the incident spatial spectrum contains predominantly propagating harmonics)? The positive answer to this question can potentially open up interesting application possibilities, especially in thermal radiation control. The present paper answers this question positively and provides experimental confirmation of the theoretical expectations.

2. GOVERNING IDEA AND PRELIMINARY SIMULATIONS

Direct experimental studies of thermal radiation into nanowire slabs are challenging, and it is desirable to find an analogous testbed setup, where the relevant physical phenomena could be explored. A prospective thermophotovoltaic system can be implemented as it is shown in Fig. 1(a). It comprises an interdigital array of nanowires forming an effective wire-medium multilayer. In accordance with our theories such wire media may transport the electromagnetic energy in a very broad frequency band from the emitter to the photovoltaic cell [10–12, 18]. As a suitable testbed experiment in a radio-frequency range, we propose to study power transport between two open ends of usual rectangular waveguides through a wire-medium slab. This is a suitable model for emulating thermal power pickup from a hot body because in the vicinity of the open end of a waveguide the field structure contains a broad mix of both propagating and evanescent waves, similarly to the modal structure of thermal oscillations in a hot body. In such scaled experiments, measurements can be done in the microwave frequency range and the dimensions and position of the wires can be easily controlled.

From the exact solution of the problem of a semi-infinite rectangular waveguide [19] it is known that at its termination the spatial spectrum of the electromagnetic field is very rich. Though at the wave distance from its ends the single-mode finite-length rectangular waveguide supports only the TE_{10}-mode, near its ends the high-order (evanescent) spatial harmonics of both TE and TM types are present, and there is no domination of TE-waves among them [19]. Introducing a WM slab in the waveguide into a certain subwavelength depth d, as it is shown in the inset of Fig. 1(b), we enable near-field interactions between the slab wires and the multi-modal fields existing close to the waveguide termination. One can say that this interaction "spreads" the electromagnetic boundary of the WM slab, although all the wires have the same length. Effectively, in the electromagnetic sense this boundary is not anymore a sharp interface. Consequently, we expect that Fabry-Perot resonances of the WM slab in this case will be suppressed. Next, this interaction results in the excitation of the WM slab by the high-order TM-modes generated at the waveguide termination. Moreover, we show that a WM slab (although it does not interact with TE-waves) enables power transfer between the incoming and outgoing waves of both polarizations, TM and TE. This is possible because at the junction between the waveguide and the WM slab the incident TE-waves can be converted into a wave package with a broad spatial spectrum
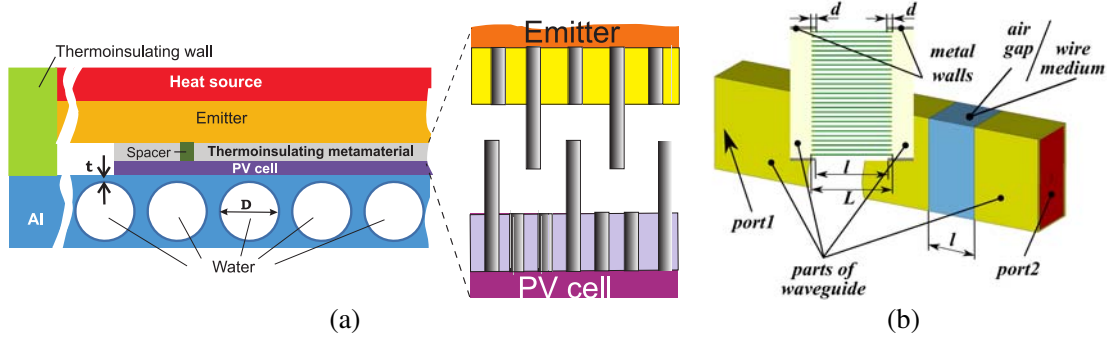
Figure 1. (a) Example of a micron-gap thermophotovoltaic system enhanced by a metamaterial. The zoom insert shows the location of nanowires between emitter and photovoltaic cell. (b) Simulated structure of two parts of an Al rectangular waveguide (with input and output ports 1 and 2) separated by a gap of length l either empty or filled by a copper WM slab of thickness $L = l + 2d$ (see the inset).

comprising a significant TM-polarized component. Then, the TE-polarized waveguide mode can be transferred through the gap filled by the WM.

In the absence of the WM slab the ends of the input and output waveguides shown in Fig. 1(b) are also coupled via radiation from the end of the input waveguide. However, this coupling is rather weak because a termination of a rectangular waveguide is a rather poor antenna in both transmission and reception regimes. If $l \ll \lambda$, there is also some near-field coupling through the air gap via evanescent waves. However, if $l > \lambda/4$, the contribution of this coupling into power transfer is negligibly small compared to the radiative (far-field) coupling.

In the presence of the WM slab near-field coupling of the waveguide terminations with the WM arises. Effective transition layers are formed at both sides of the gap. In these transition layers propagating and evanescent eigenmodes of the WM effectively interact with the high-order eigenmodes of the waveguide. Since the WM is a spatially dispersive material, Maxwell's boundary conditions are not sufficient to calculate the power transfer and additional boundary conditions (ABC) are necessary. ABC on the surface of a WM slab do not prohibit conversion of the incident TE-wave into TM-waves if the environment of the slab is inhomogeneous [20]. Though for a WM slab located in free space this conversion does not occur [21], it becomes possible in our case when the WM slab overlaps with the open waveguide edges. We did not derive ABC for this difficult case, however, we have numerically simulated the electric field distributions which confirmed the mode conversion effect. We saw this effect in a vector color map and expect that it will result in a noticeable enhancement of power transfer (which should be broadband, because is not resonant). In this regime, the WM slab will be efficiently excited by the incident TE_{10}-mode of the input waveguide and will symmetrically excite the TE_{10}-mode in the output one, although the wires are directed orthogonally to the electric field of the fundamental waveguide mode.

Theoretical estimations of the optimal value of the overlapping length d which grants this favorable regime are rather challenging. Therefore, we have studied this issue performing a series of numerical simulations. To make the numerical model as close to the reality, we took into account the finite conductivity of both the waveguide walls and the wires. Numerical simulations were implemented using CST Studio Suite for a rectangular waveguide with Al walls whose dimensions $a = 164$ mm and $b = 82$ mm imply the cutoff frequency for the TE_{10}-mode at 0.9 GHz. The single-mode regime of this waveguide holds within the frequency range 0.9–2 GHz. The thickness of copper wires (1.5 mm) and the lattice period of WM (6 mm) were chosen in accordance to the recommendations of work [22], so that the copper filling factor is equal to 0.125.

Figure 2 illustrates the simulation results for an empty gap and the gap filled by a WM slab with different values of d and fixed $l = 90$ mm. Here the thickness L of the WM sample varies accordingly, i.e., $L = l + 2d$. The contrast with the case of the empty gap is explicitly seen. The air gap 90 mm is larger than the quarter-wavelength in the range 1–2 GHz, which does not allow any noticeable near-field coupling between the input and output waveguides. The power in the output waveguide results only
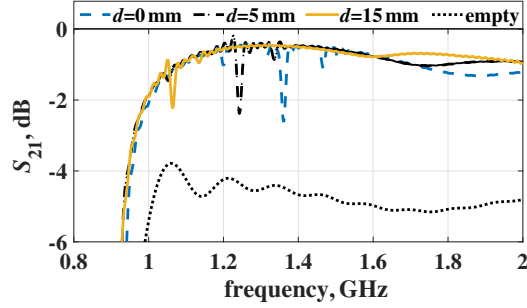
Figure 2. S_{21}-parameter, simulated for the gap $l = 90$ mm, empty or filled with the WM for different values of $d = 0, 5, 15$ mm.

(a) (b)
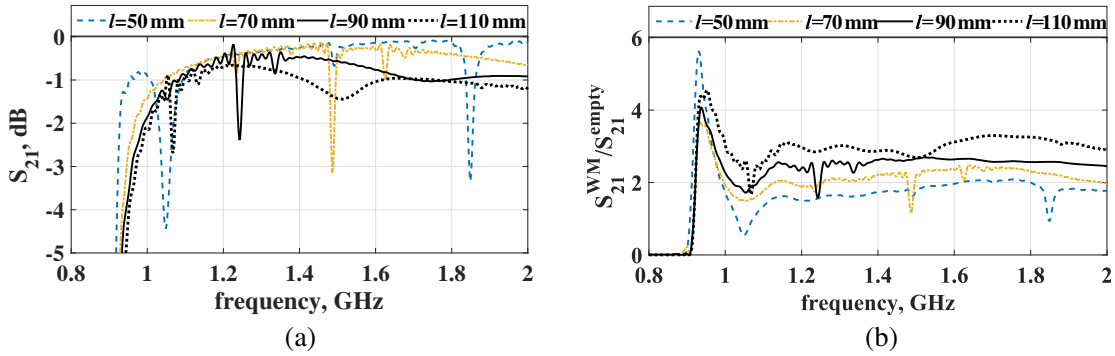
Figure 3. Simulation results, obtained for the model with WM slab with $d = 5$ mm and $l = 50, 70, 90$ and 110 mm: (a) absolute value of the power transmittance; (b) gain in power transmittance due to WM $S_{21}^{WM}/S_{21}^{empty}(f)$.

from the radiation from the end of the input waveguide and is nearly 3.5 times smaller than the power in the input waveguide (in the range 1–2 GHz). The WM slab inserted into the gap increases the power transmittance in this frequency range nearly 2.5 times. One can see that the curves of S_{21} for $d = 0$–15 mm are close to one another. They differ only by the frequency at which the (rather weak) resonant reflection is observed (1.05, 1.25 and 1.35 GHz, respectively). Therefore, in our further simulations the value d is taken equal to 5 mm.

The next series of simulations was performed for $d = 5$ mm and different values of $l = 50, 70, 90$, and 110 mm. With the presence of the WM slab the averaged value of $|S_{21}|$ in the range 1–2 GHz grows when l decreases, see Fig. 3(a). However, the enhancement of the power transfer granted by WM slab is better for higher values of l. Fig. 3(b) illustrates the frequency dependence of the gain in the power transfer $S_{21}^{WM}/S_{21}^{empty}(f)$. The WM slab replacing the air gap multiplies the power transmittance 2–3 times except the narrow frequency range just above the cutoff. In this band the coupling of the output and input parts of the waveguide through the air gap is very weak (S_{21} is less than -20 dB), and the presence of the WM turns out to be the most useful.

3. EXPERIMENTAL AND NUMERICAL STUDY OF THE POWER TRANSFER THROUGH THE GAP BETWEEN TWO WAVEGUIDES AT LOW FREQUENCIES

For the experimental study of the enhancement effect a WM slab with the length of $L = 100$ mm was manufactured. Foam blocks were used for ensuring the structural integrity. We checked that they practically do not affect the power transfer in the absence of wires. The values $l = 90$ mm and $d = 5$ mm were selected according to our preliminary simulations. The experimental setup is shown in Fig. 4. The first part of our experiment refers to the range 0.9–2 GHz, where the input and output waveguides are

single-mode ones.

The waveguide experiment allowed us to verify that evanescent waves strongly contribute to power transfer through the conversion into propagating eigenmodes of the WM slab. With this purpose we introduced a dense wire grid (square-cell metal mesh) near the end of the input waveguide as it is shown in Fig. 4(b). Mutual location of the grid and the WM slab is illustrated by Fig. 5.

In the absence of the WM the grid blocks the propagating mode and creates high-order evanescent ones. These waves attenuate behind the grid at the distance which nearly equals to the mesh period $p = 1\,\mathrm{cm}$. If the distance $\delta + d$ between the grid and the waveguide termination is not much larger than p, evanescent waves still excite the end of the input waveguide and the coupling of the input and output waveguides though weak is still detectable even in the absence of the WM. In the presence of the WM these evanescent waves should partially convert into propagating eigenmodes and increase the power transfer. Notice, that in the canalization regime these waves convert back to the evanescent waves at the rear side of the WM slab. Therefore, the canalization regime would be not helpful for our purposes even at the frequency of the Fabry-Perot resonance. However, the regime which we study here is very different from canalization. In the present case there is an effective transition layer at the rear interface of the WM slab. Over this layer the eigenmodes of the WM efficiently couple to the TE$_{10}$-mode of the output waveguide. Therefore, even if the propagating incident wave is blocked, the WM slab still increases the power transfer in the broad band.


(a)   (b)   (c)
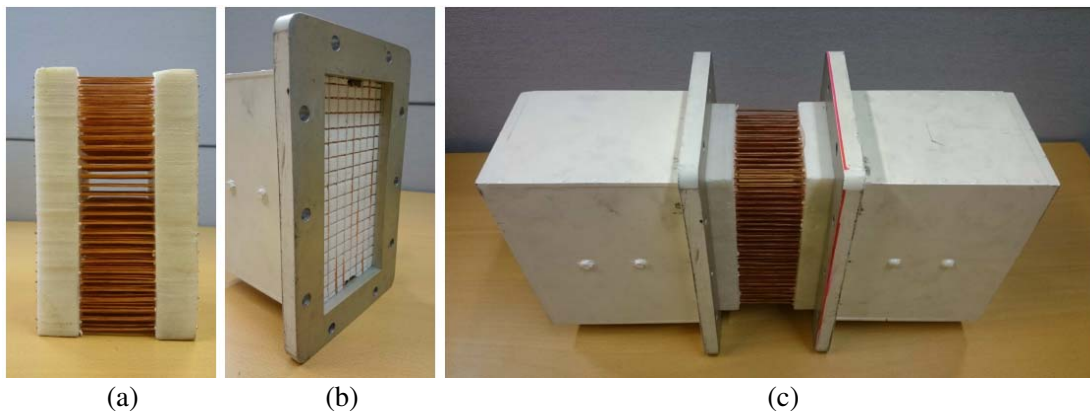
Figure 4. The experimental setup: (a) our wire medium slab; (b) the grid near the edge of the input waveguide; (c) the external view of our setup.


(a)   (b)
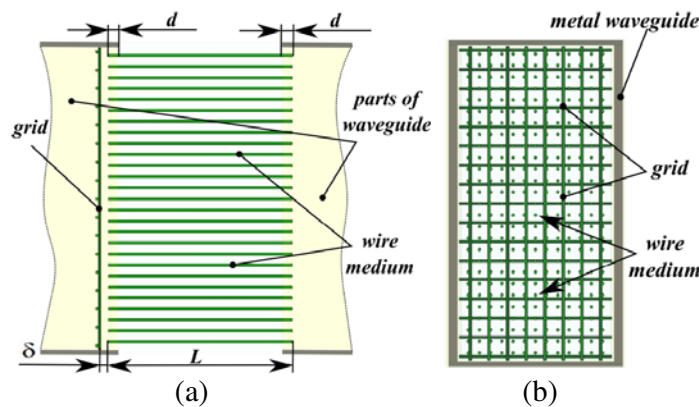
Figure 5. The WM slab inserted between the input and output waveguides is complemented by the wire grid with square cells. The structure is shown in the (a) longitudinal and (b) transverse cross-sections of the waveguide.

The frequency dependencies of S_{21} in the range 0.8–2 GHz (recall that in the range 0.9–2 GHz the single-mode regime holds in the input and output waveguides) are shown in Figs. 6 and 7. Fig. 6 corresponds to the absence of the grid and Fig. 7 corresponds to its presence (see Fig. 5). Inspecting Figs. 6(a) and 6(c) we can notice that the measured values of S_{21} in both cases of the gap filling (empty gap and gap filled with the WM) match well with the simulations except the narrow band of resonant reflection around 1.9 GHz. This resonance is probably related to mode interference. The two-mode regime theoretically starts at 2 GHz, however, the modification of the waveguide by our insertions may somewhat shift this frequency. The gain granted by the WM slab illustrated in Figs. 6(b) and 6(d) (simulations and measurements, respectively) is definitely broadband. The resonant peak at 0.85 GHz in Fig. 6(d) is below cut-off, and the peak at 1.9 GHz has been already commented. In the range 0.9–2 GHz the simulation shows that the averaged gain nearly equals to 2.5, whereas the measurements give the averaged gain close to 2.

The broadband power transfer enhancement assisted by WM remains strong in the case when the source waveguide produces only evanescent waves. Inspecting Fig. 7 it is easy to notice quite strong disagreement between simulated and measured data. Actually, these simulations do not reveal numerous and strong resonances of reflection and transmission and significantly underestimate the power transfer through the gap. The reason is that the used software has turned out to be not adequate for calculating so tiny structures as the grid, the WM and the edges of the waveguide walls, strongly coupled by near fields. Attempts to increase the computation accuracy did not allow us to keep the computation time reasonable. However, the gain in the power transfer granted by the WM is simulated rather adequately. Simulations predict that this gain averaged over the range 0.9–2 GHz is close to 3.0, while the measurements give the value 2.24.
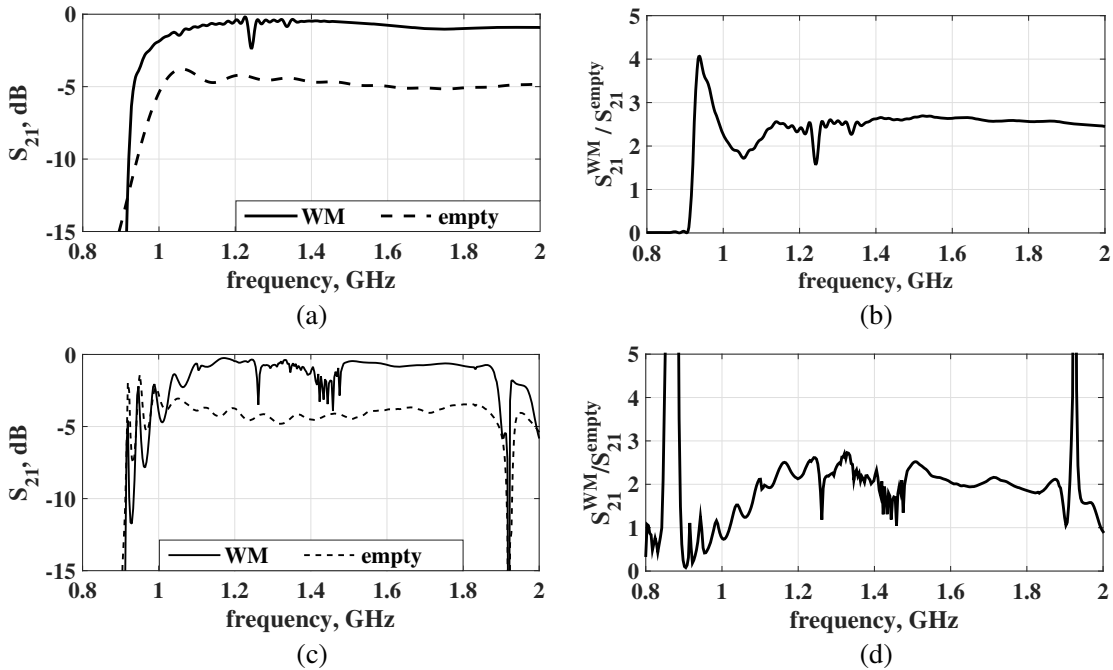
Figure 6. Results for the power transmittance through the gap $l = 90$ mm between two waveguides either filled with the WM or empty, and for the gain in the power transfer due to the WM slab: (a) simulated S_{21}; (b) simulated $S_{21}^{\mathrm{WM}}/S_{21}^{\mathrm{empty}}$; (c) measured S_{21}; (d) measured $S_{21}^{\mathrm{WM}}/S_{21}^{\mathrm{empty}}$.
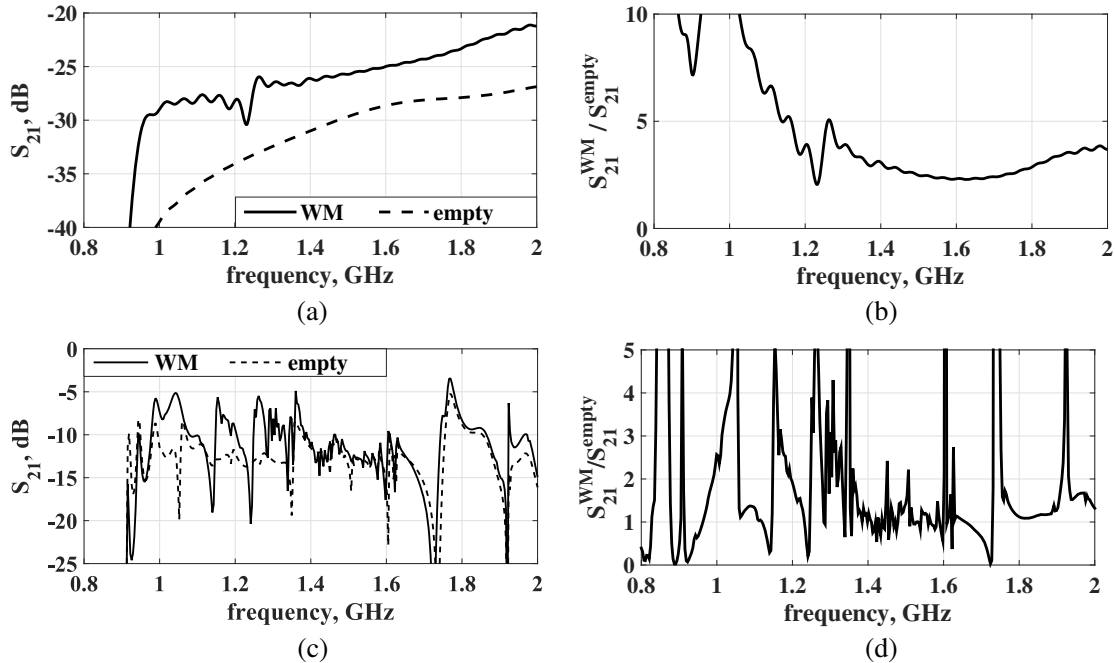
Figure 7. The same plots as in 6 for the case when the wire mesh is inserted at the distance $\delta = d = 5$ mm from the interface of the WM slab.

## 4. EXPERIMENTAL STUDY OF THE POWER TRANSFER THROUGH THE GAP BETWEEN TWO WAVEGUIDES UP TO 12 GHz

If the waveguide is multi-modal, i.e., its spatial spectrum is rich, interactions of overlapping fields in the waveguide and the WM in the transition layer should be more efficient and the power transfer in the slab should increase once more. To check this hypothesis we made the same measurements as above in the frequency range 0.9–12 GHz. Numerical simulations with the wire medium slab (and especially with the square mesh) for this band would consume huge computational resources and we omitted them. In Figs. 8 and 9 we present the experimental high-frequency data for the same configurations as in Figs. 6(c) and (d) and Figs. 7(c) and (d). Mode interference in this frequency range creates multiple transmittance resonances which make the original frequency plots difficult for visual analysis. Thus, we plot smoothed S_{21}-parameter plots, using the cubic spline method. In accordance to the data presented in Fig. 8(b), the frequency-averaged gain in the frequency band 0.9–12 GHz is equal to 3.78.

When the grid is inserted and the end of the input waveguide is excited only by evanescent waves, the impact of the WM slab is stronger. In accordance to Fig. 9(b), the averaged gain in this case equals 4.44. This result agrees with that obtained for the single-mode regime in the input waveguide. The smoothed gain weakly oscillates versus frequency with the general increasing trend. This result is not surprising since at high frequencies the gap becomes wider as compared to the wavelength.

5. DISCUSSION AND CONCLUSIONS

The main purpose of this paper is to validate the very concept of broadband power transfer through bunches of thin conductors. Here we have proved (to our knowledge, for the first time) that the WM is capable to enhance broadband power transfer in both principal cases: when it is excited by propagating waves and when it is excited by evanescent waves. This property can be important for prospective systems harvesting and/or transmitting electromagnetic energy at long distances, picking up power from both propagating and evanescent modes of the source field.

Our experimental study has confirmed this effect which may find applications in a number of
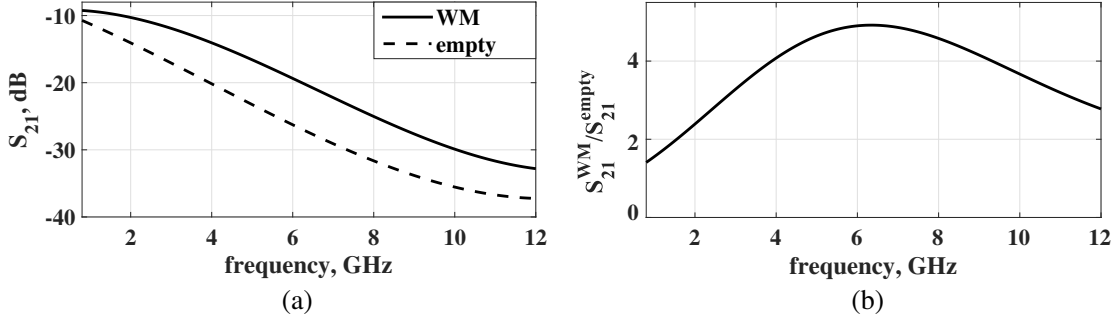
Figure 8. The smoothed experimental transmittance with WM, without WM and the gain due to the WM in the frequency range from 0.9 to 12 GHz: (a) S_{21} (logarithmic scale); (b) $S_{21}^{WM}/S_{21}^{empty}$.
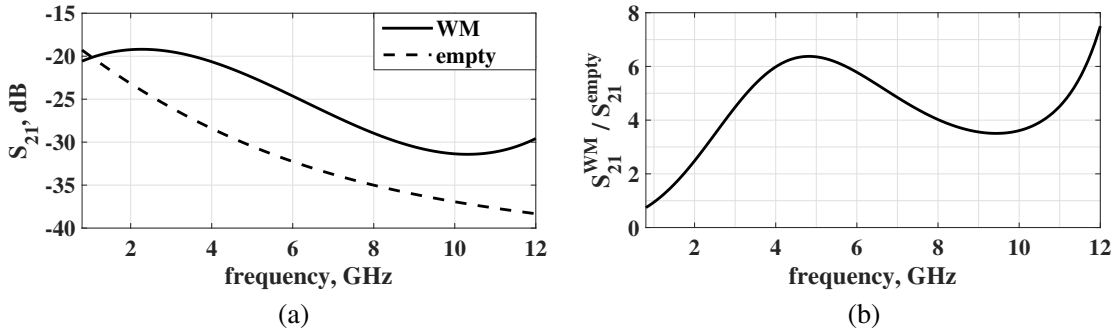
Figure 9. The same plots as in 8 for the case when the grid is inserted at the distance $\delta + d$ from the end of the input waveguide.

different devices. First of all, it is important for further development of thermophotovoltaic systems enhanced by nanowires, which were reviewed in Introduction. Our experiment mimics one of key features of these prospective systems: the multi-mode, long-distance and broadband transport of electromagnetic energy through the WM slab. The most known objection to expensive experiments with these systems is that such slabs cannot efficiently transfer the electromagnetic energy beyond their thickness resonances. Here, this objection has been successfully refuted experimentally. We have shown that a WM slab whose one side is submerged into a waveguide, efficiently transmits a broad spectrum of electromagnetic energy to another side. Therefore, a WM slab whose one side is submerged into a hot dielectric medium should transmit the whole radiative heat to its cold side, as it was theoretically predicted in [10].

The metal waveguide of the present work is an analogue of a dielectric thermal emitter. In both cases the near-field interaction of the wire ends with the waveguide edge/dielectric surface results in a transition layer formed at the corresponding side of the wire-medium slab. This strongly subwavelength layer is responsible for the efficient and broadband multimode excitation of the WM by the electromagnetic waves incoming from the input waveguide/dielectric medium. This transition layer spreads the boundary of the WM slab and damps its thickness resonances.

In our work an efficient power transfer has been experimentally shown for the case when the WM slab is excited by evanescent waves. This experiment mimics the part of radiative heat transfer which in the theory [10, 11] is carried out by evanescent waves converted in the WM into propagating modes. In the theory of thermophotovoltaic systems the Planckian radiative heat transfer is defined as the power flux transferred from the hot medium by propagating waves. This flux is restricted by the so-called black-body limit. The involvement of evanescent spatial spectrum into radiative heat transfer theoretically allows one to beat this limit achieving the so-called super-Planckian radiative heat transfer [13–15]. In our earlier works [10–12] it was theoretically shown, that this involvement is very efficient when it is implemented by WM. In the present paper we have shown experimentally the conversion of evanescent waves into propagating ones at the sides of the wire-medium slab. This effect

was previously demonstrated experimentally only at the frequencies of the thickness resonance, together with the imaging in the WM superlens. We have experimentally demonstrated this conversion beyond any resonance, in a very broad frequency range. This is a strong argument in favor of super-Planckian radiative heat transfer in thermophotovoltaic systems enhanced by nanowires.

Thus, our expectations, in what concerns the coupling of the WM slab with the mixture of propagating and evanescent modes of an emitter, have been confirmed. Moreover, the near-field coupling between the waveguide termination and the interface of the WM slab results in conversion of TE modes into a spectrum of TE and TM-modes. This makes a WM slab interesting for some other applications, related with telecommunications. It is known that WM endoscopes maintain their effectiveness even if the arrays of wires are tapered [8, 9] or bent [22]. Therefore, WM endoscopes can be, probably, used for coupling two hollow waveguides of different dimensions or located at some angle to one another. These applications would require further experiments.

A surprising feature of the near-field coupling between the interface of the WM slab and the waveguide edge is that the value of the overlapping d is not important under the condition $d \ll \lambda$. For any sufficiently small positive d we observe strong coupling of the WM and the waveguide. Notice, that if $d < 0$ (no overlapping), the WM slab is excited extremely weakly and only decreases the power transfer (reflecting the radiation from the open end of the input waveguide). This conclusion agrees with the results of papers [10–12], where it was proposed to embed the wires into the radiating hot body in order to ensure effective excitation of the wire medium sample.

In addition, we have studied enhancement of power transfer utilizing specially prepared bianisotropic scatterers, so-called wire omega particles (see e.g., in monograph [23]) which partially convert TE waves into the TM ones. However, the introduction of these particles does not increase the frequency-averaged power transfer. Due to their resonant nature, at some frequencies these particles enhance the coupling but at other frequencies they produce additional reflections back into the source waveguide. Transition layers obtained by a small overlapping of the WM sample and the TE-mode waveguide, in general, offer better coupling to the TE-mode, since in this case there are no resonant elements in the system.

To conclude, with the obtained numerical and experimental results we have confirmed that WM slabs effectively enable broadband power transfer which occurs beyond Fabry-Perot resonances. Moreover, interfaces of WM slabs can be efficiently coupled to TE-polarized waves on condition of properly organized transition layers at these interfaces. The results of this study are relevant, for example, to applications in enhancing and controlling radiative heat flow, especially in thermophotovoltaic systems, and in creating effective multi-mode telecommunication antennas.

ACKNOWLEDGMENT

REFERENCES

1. Simovski, C. R., P. A. Belov, A. V. Atrashchenko, and Yu. S. Kivshar, "Wire metamaterials: Physics and applications," *Adv. Mater.*, Vol. 24, 4229–4248, 2012.

2. Belov, P. A., R. Marques, S. I. Maslovski, I. S. Nefedov, M. Silverinha, C. R. Simovski, and S. A. Tretyakov, "Strong spatial dispersion in wire media in the very large wavelength limit," *Phys. Rev. B*, Vol. 67, 113103(1–4), 2003.

3. Nefedov, I. S. and A. J. Viitanen, "Wire media," *Metamaterial Handbook. Vol. 1: Theory and Phenomena of Metamaterials*, Chapter 15-1, CRC Press, Boca Raton, 2009.

4. Simovski, C. R. and P. A. Belov, "Low-frequency spatial dispersion in wire media," *Phys. Rev. E*, Vol. 70, 046616(1–8), 2004.

5. Belov, P. A., C. R. Simovski, and P. Ikonen, "Canalization of subwavelength images by electromagnetic crystals," *Phys. Rev. B*, Vol. 71, 193105(1–4), 2005.

6. Belov, P. A., Y. Zhao, S. Sudhakaran, A. Alomainy, and Y. Hao, "Experimental study of the subwavelength imaging by a wire medium slab," *Appl. Phys. Lett.*, Vol. 89, 262109, 2006.

7. Belov, P. A., Y. Zhao, S. Tse, P. Ikonen, M. G. Silveirinha, C. R. Simovski, S. A. Tretyakov, Y. Hao, and C. Parini, "Transmission of images with subwavelength resolution to distances of several wavelengths in the microwave range," *Phys. Rev. B*, Vol. 77, 193108, 2008.

8. Shvets, G., S. Trendafilov, J. B. Pendry, and A. Sarychev, "Guiding, focusing, and sensing on the subwavelength scale using metallic wire arrays," *Phys. Rev. Lett.*, Vol. 99, 053903, 2007.

9. Zhao, Y., G. Palicaras, P. A. Belov, R. F. Dubrovka, C. R. Simovski, Y. Hao, and C. G. Parini, "Magnification of subwavelength field distributions using a tapered array of metallic wires with planar interfaces and an embedded dielectric phase compensator," *New J. Phys.*, Vol. 12, 103045, 2010.

10. Nefedov, I. S. and C. R. Simovski, "Giant radiation heat transfer through micron gaps," *Phys. Rev. B*, Vol. 84, 195459, 2011.

11. Maslovski, S. I., C. R. Simovski, and S. A. Tretyakov, "Equivalent circuit model of radiative heat transfer," *Phys. Rev. B*, Vol. 87, 155124, 2013.

12. Mirmoosa, M. S., F. Ruting, I. S. Nefedov, and C. R. Simovski, "Effective-medium model of wire metamaterials in the problems of radiative heat transfer," *J. Appl. Phys.*, Vol. 115, 234905, 2014.

13. Simovski, C., S. Maslovski, I. Nefedov, and S. Tretyakov, "Optimization of radiative heat transfer in hyperbolic metamaterials for thermophotovoltaic applications," *Opt. Express*, Vol. 21, 14988–15013, 2013.

14. Guo, Y., C. L. Cortes, S. Molesky, and Z. Jacob, "Broadband super-Planckian thermal emission from hyperbolic metamaterials," *Appl. Phys. Lett.*, Vol. 101, 131106, 2012.

15. Pendry, J. B., "Radiative exchange of heat between nanostructures," *J. Phys.: Condens. Matter*, Vol. 11, 6621, 1999.

16. Chang, J.-Y., Y. Yang, and L. Wang, "Tungsten nanowire-based hyperbolic metamaterial emitters for near-field thermophotovoltaic applications," *Int. J. Heat Mass Tran.*, Vol. 87, 237, 2015.

17. Ilic, O., M. Jablan, J. D. Joannopoulos, I. Celanovic, and M. Soljačić, "Overcoming the black body limit in plasmonic and graphene near-field thermophotovoltaic systems," *Opt. Express*, Vol. 20, A366–A384, 2012.

18. Mirmoosa, M. S. and C. Simovski, "Micron-gap thermophotovoltaic systems enhanced by nanowires," *Photon. Nanostruct. Fundam. Appl.*, Vol. 13, 20–30, 2014.

19. Bois, K. J., A. D. Benally, and R. Zoughi, "Multimode solution for the reflection properties of an open-ended rectangular waveguide radiating into a dielectric half-space: The forward and inverse problems," *IEEE Trans. Instr. Meas.*, Vol. 48, 1131, 1999.

20. Hanson, G. W., M. G. Silveirinha, P. Burghignoli, and A. B. Yakovlev, "Non-local susceptibility of the wire medium in the spatial domain considering material boundaries," *New J. Phys.*, Vol. 15, 083018, 2013.

21. Belov, P. A. and M. G. Silveirinha, "Resolution of subwavelength transmission devices formed by a wire medium," *Phys. Rev. E*, Vol. 73, 056607, 2006.

22. Radu, X., D. Garray, and C. Craeye, "Toward a wire medium endoscope for MRI imaging," *Metamaterials*, Vol. 3, 90–99, 2009.

23. Serdyukov, A. N., I. V. Semchenko, S. A. Tretyakov, and A. Sihvola, *Electromagnetics of Bi-anisotropic Materials: Theory and Application*, Gordon and Breach Science Publishers, Amsterdam, 2001.